In Vivo Intracellular pH Measurements in Tobacco and *Arabidopsis* Reveal an Unexpected pH Gradient in the Endomembrane System[W]

Alexandre Martinière,[a] Elias Bassil,[b] Elodie Jublanc,[c] Carine Alcon,[a] Maria Reguera,[b] Hervé Sentenac,[a] Eduardo Blumwald,[b] and Nadine Paris[a,1]

[a] Biochemistry and Plant Molecular Biology Lab, Unité Mixte de Recherche 5004, 34060 Montpellier, France
[b] Department of Plant Sciences, University of California, Davis, California 95616
[c] Institut National de la Recherche Agronomique, Unité Mixte de Recherche 866, Dynamique Musculaire et Métabolisme, 34060 Montpellier, France

The pH homeostasis of endomembranes is essential for cellular functions. In order to provide direct pH measurements in the endomembrane system lumen, we targeted genetically encoded ratiometric pH sensors to the cytosol, the endoplasmic reticulum, and the *trans*-Golgi, or the compartments labeled by the vacuolar sorting receptor (VSR), which includes the *trans*-Golgi network and prevacuoles. Using noninvasive live-cell imaging to measure pH, we show that a gradual acidification from the endoplasmic reticulum to the lytic vacuole exists, in both tobacco (*Nicotiana tabacum*) epidermal (ΔpH −1.5) and *Arabidopsis thaliana* root cells (ΔpH −2.1). The average pH in VSR compartments was intermediate between that of the *trans*-Golgi and the vacuole. Combining pH measurements with in vivo colocalization experiments, we found that the *trans*-Golgi network had an acidic pH of 6.1, while the prevacuole and late prevacuole were both more alkaline, with pH of 6.6 and 7.1, respectively. We also showed that endosomal pH, and subsequently vacuolar trafficking of soluble proteins, requires both vacuolar-type H^+ ATPase–dependent acidification as well as proton efflux mediated at least by the activity of endosomal sodium/proton NHX-type antiporters.

INTRODUCTION

Luminal pH of distinct intracellular compartments of the endomembrane system is homeostatically maintained. In animals, the pH of specific intracellular compartments along the endocytic pathway has been measured and shown to be progressively more acidic (Casey et al., 2010; Ohgaki et al., 2011). In plants, however, while pH values of the cytosol, vacuole, and apoplast have been reported, no measurements are available for the endoplasmic reticulum (ER), Golgi, *trans*-Golgi network (TGN), or late endosomes/prevacuolar compartment (PVC)/multivesicular body (MVB). Many studies indirectly support the existence of a pH gradient within the plant secretory pathway. Treatment with monensin, a monovalent ion-selective ionophore known to collapse proton gradients, causes alterations in the morphology of the *trans* face of the Golgi apparatus in plants similar to those reported in animal cells (Mollenhauer et al., 1990). It was suggested that the effect of monensin on membrane trafficking within the secretory pathway was likely due to acidification of the TGN (Boss et al., 1984). Later, it was shown that disrupting the proton gradient with monensin impaired vacuolar transport of soluble proteins such as phytohemagglutinin (Gomez and Chrispeels,

1993) or storage protein precursors (Matsuoka et al., 1990). Protein secretion is also affected by monensin, as shown in sycamore (*Acer pseudoplatanus*) suspension cells (Zhang et al., 1993).

Proton pumps, such as the vacuolar-type H^+ ATPases (V-ATPases) and pyrophosphatase constitute the primary active mechanism to acidify intracellular organelles (Schumacher, 2006; Marshansky and Futai, 2008). Two inhibitors of V-ATPases, bafilomycin A and concanamycin A, used to examine the role of these proton pumps on protein transport, lead to the secretion of soluble vacuolar proteins, the retention of secreted proteins (Matsuoka et al., 1997), and blocking of the endocytosis tracer FM4-64 (Dettmer et al., 2006). Monensin, bafilomycin A, and concanamycin A induce massive changes in Golgi morphology with an increase of saccules and an accumulation of vesicles at the *trans* face of the Golgi (Dettmer et al., 2006; Scheuring et al., 2011). Recently, endosomal NHX-type Na^+/H^+ antiporters have been proposed to play a role in maintaining pH homeostasis (Bassil et al., 2011a, 2012), as other cation/H^+ exchangers do (reviewed in Chanroj et al., 2012). In mammalian cells, NHX-type antiporters have been suggested to function as proton leaks to counterbalance luminal acidification generated by V-ATPases (Demaurex, 2002; Orlowski and Grinstein, 2007).

Indirect evidence for a role of organelle acidification in vacuolar transport was also provided by in vitro binding assays between the vacuolar sorting receptor (VSR) and its ligand, the vacuolar sorting determinants of 12S globulin, and the protease aleurain (Kirsch et al., 1994; Ahmed et al., 2000; Shimada et al., 2003b). It was reported that binding occurred at pH 7.0 and was abolished at pH 4, with optimal binding occurring at pH 6.0 (Kirsch et al.,

1994). A current model proposes that binding of the receptor to the vacuolar proprotein occurs in the TGN (daSilva et al., 2005; Saint-Jean et al., 2010) and is abolished in the PVC where the pH is predicted to be more acidic (Foresti et al., 2010; Saint-Jean et al., 2010).

By contrast, few direct measurements of the luminal pH of compartments of the plant secretory pathway have been attained using pH-sensitive fluorescent dyes. Membrane-permeable ratiometric fluorescent dyes such as acetoxymethyl ester of 2',7'-bis-(2-carboxyethyl)-5-(and-6)-carboxyfluorescein (BCECF-AM) or Lysosensor have been used in plants to measure pH of the vacuole and gave an average vacuolar pH of 5.5 (Brauer et al., 1995; Matsuoka et al., 1997; Otegui et al., 2006; Krebs et al., 2010; Bassil et al., 2011a; Fukao and Ferjani, 2011). In *Arabidopsis thaliana* leaves, the central vacuole has a pH of 6, while senescence-associated vacuoles are more acidic (Otegui et al., 2005). Nevertheless, the use of fluorescent dyes is not suitable for measuring pH in smaller intracellular compartments, such as the Golgi. Recent advances in live imaging and the development of genetically encoded fluorescent protein sensors provide new tools needed to directly and noninvasively measure the luminal pH in diverse cellular compartments of plant cells in vivo. pHluorin, a pH-sensitive variant of green fluorescent protein (GFP), has been used to measure the pH of vesicles during endocytosis or exocytosis events in living mammalian cells (Miesenböck et al., 1998; Tsuboi and Rutter, 2003). In plants, pHluorin has been used to measure cytosolic and apoplastic pH in response to various abiotic stresses (Moseyko and Feldman, 2001; Gao et al., 2004). Recently, optimized pH sensors have also been developed (Schulte et al., 2006; Gjetting et al., 2012).

In this study, we developed a set of genetically encoded, pHluorin-based pH sensors targeted to specific endomembrane compartments, and used quantitative live-cell imaging to measure the luminal pH in a noninvasive manner. We show the existence of a pH gradient within the secretory pathway with the ER being the most alkaline and the vacuole the most acidic. Surprisingly, the luminal pH in the TGN was more acidic than in the PVC/MVB and even in the late PVC. We also show that luminal pH homeostasis in TGN and PVC involved both V-ATPase–dependent acidification and proton efflux mediated potentially by the activity of NHX-type antiporters.

RESULTS

The Ratiometric pH Sensor pHluorin Is Insensitive to Ionic Changes Other Than the Proton Concentration

The lumen of plant cellular compartments can vary greatly in their ionic composition or reducing environment. To examine the possible influence of various luminal conditions on pH, we produced recombinant pHluorin from bacteria and tested whether several ionic and chemical conditions affected the pH calibration of pHluorin. As previously reported (Miesenböck et al., 1998), a sigmoidal fluorescence ratio response of pHluorin was found when it was incubated with buffers of different pH (Figure 1A). The portion of the calibration curve around pH 6, enlarged in Figure 1B, showed that pHluorin is suitable for pH measurement at most down to pH 5.5. We also tested highly reducing conditions, high

concentrations of salts, such as NaCl, KCl, and $CaCl_2$, as well as hydrogen peroxide and found than none of these treatments affected substantially the shape of the calibration curve (Figure 1A). This suggests that pHluorin is suitable for pH measurements in diverse intracellular compartments and conditions.

Targeted pHluorin Localized to Distinct Subcellular Compartments of the Secretory Pathway

In order to target the ratiometric pH sensor to the lumen of specific compartments, we chose proteins whose localization and topology are well characterized and generated translational fusion proteins with pHluorin. The compartment-specific pH sensors developed in this study are listed in Table 1 and explained in detail in the Methods. All experiments were performed both in transiently expressing tobacco (*Nicotiana tabacum*) epidermal cells and in stably expressing *Arabidopsis*. The fluorescence patterns and subcellular localization of each pH sensor were typical for their corresponding cellular compartments in both tobacco epidermal cells (Figure 2A) and *Arabidopsis* root cells (see Supplemental Figure 1A online). As already shown for GFP (Tamura et al., 2003), pHluorin could not be detected in the central vacuole when plants were grown under light conditions. Instead, vacuolar pH was measured using the ratiometric pH sensitive dye BCECF-AM, as previously reported (Krebs et al., 2010; Bassil et al., 2011a). Given that pHluorin quenching occurs at acidic pH, we wanted to ensure that all VSR compartments would be detected, as these are predicted to be the most acidic after the vacuole. We therefore coexpressed pH-VSR together with the same VSR protein (At-VSR2;1) fused to Tag-RFP (for red fluorescent protein), a fluorescent protein that is more resistant to irreversible acidic quenching (Merzlyak et al., 2007). As shown in Figure 2B, pH-VSR and Tag-RFP-VSR colocalized.

In order to quantify colocalization, we evaluated the resolution of the imaging system and its capacity to distinguish between truly colocalized compartments and those that are associated (possibly maturing) or entirely distinct. For this purpose, we performed measurements using fluorescent beads of 500 nm in diameter or markers of the *cis*-Golgi KDEL receptor (ERD2) and the *trans*-Golgi sialyl transferase (ST; see Methods and Supplemental Figure 2 online). These control experiments indicated that the optical resolution of the imaging system was high enough to assign true colocalization as one that occurs when the distance between the centroid of two bodies was 125 nm or less. Given that the mean radius of VSR-positive organelles is 450 nm, we arbitrarily set the maximal distance at which we considered two compartments to be associated as 500 nm.

Using this colocalization approach, we found that only 7% of Tag-RFP–labeled VSR compartments were devoid of pHluorin labeling (Figure 2C). This percentage is not likely due to acidic quenching of pH-VSR since we obtained a similar result (10%) when ST-RFP and ST-pH colocalization was analyzed in similar experiments (see Supplemental Figure 2B online).

The Lumens of the Compartments along the Secretory Pathway Are Progressively More Acidic

To validate the robustness of our pH measurement approach, we first compared vacuolar pH values obtained with either the dye
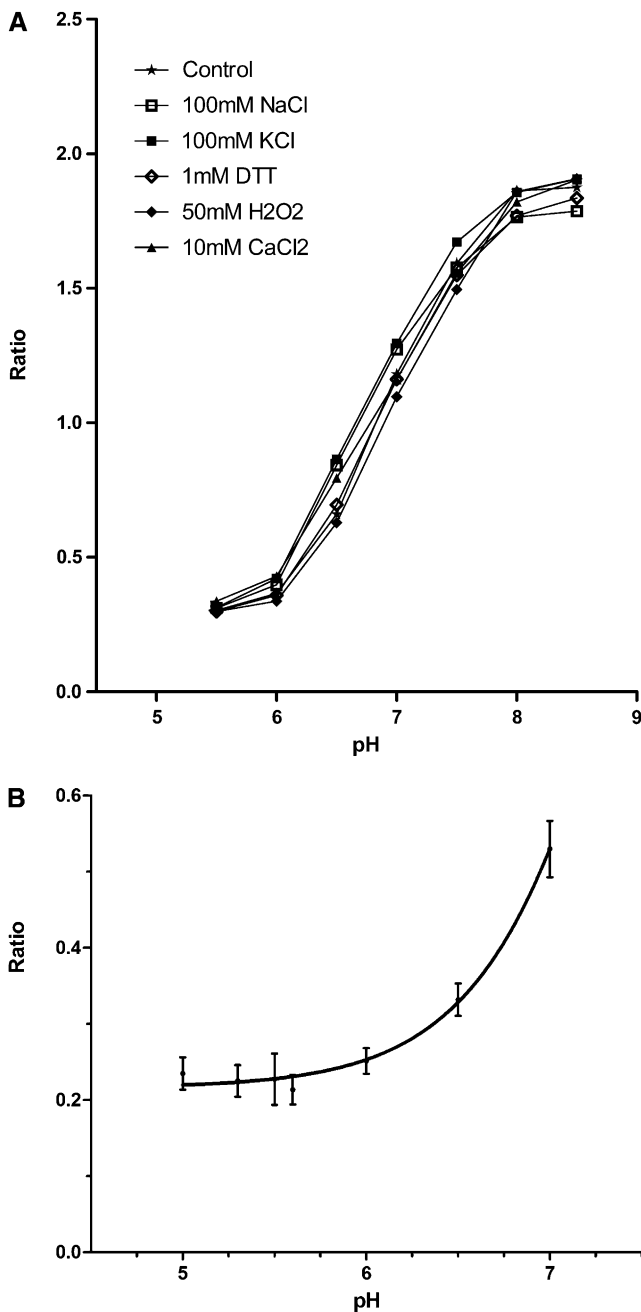
Figure 1. In Vitro Calibration of pHluorin.

pH-dependent fluorescence of bacterial recombinant pHluorin was measured using a spectrofluorometer in the presence of a series of 50 mM buffers of either MES-KOH or HEPES-KOH at different pH levels.
(A) Effect of ionic environment on the pH calibration of pHluorin; buffer only (star), with the addition of 100 mM NaCl (open squares), 100 mM KCl (closed squares), 1 mM DTT (open diamonds), 50 mM hydrogen peroxide (H_2O_2) (closed diamonds), or 10 mM $CaCl_2$ (closed triangles).
(B) Detailed calibration curve in the range of pH from 5 to 7.

BCECF-AM or pHluorin fused to aleurain (Aleu-pH) expressed in plants incubated in the dark. We found that pH measurements obtained with both sensors were similar under the same conditions (see Supplemental Figures 3A and 3B online). Secondly, and in order to rule out possible effects of fusion proteins on pH quantification, we compared the pH values in pH-HDEL– and pH-ST–positive compartments when luminal pH was equilibrated using buffers of pH 5.5 or 8.5 (see Supplemental Figure 4 online). We found no strong effect of the fusion proteins on pH. Interestingly, we also observed that buffer pH 5.5 failed to impose a proton equilibrium between the outside media and intracellular lumen (see Supplemental Figure 4 online). For this reason, we favored an in situ calibration approach, as previously described in plants (Gao et al., 2004; Schulte et al., 2006). Third, we tested the stability of pH measurements over the duration of confocal imaging in which plants were maintained in dim light conditions. As shown in Figure 2D, the pH remained stable (pH 6.5) during the imaging period even though pH-VSR exhibited a much more alkaline pH when measured in plants that were maintained in darkness during the entire transient expression period of 2 d.

In tobacco leaves and in *Arabidopsis* roots, we found that the secretory pathway was more acidic than the cytosol (Figure 3; see Supplemental Figure 1B online). We observed a ΔpH of −1.5 and −2.1 between the more neutral ER lumen and that of the more acidic vacuole in tobacco (Figure 3) and in *Arabidopsis* (see Supplemental Figure 1B online). Even though some variations of pH could be observed within a given subpopulation of organelles, the average pH remained significantly different between different categories of compartments (Tukey test, P value < 0.001; Figure 3). The acidification appeared to be gradual, with a difference of roughly 0.5 units between each category of the cellular compartments that were measured, such that pH-VSR–positive compartments harbored a pH lower than that of the *trans*-Golgi but higher than that of the vacuole.

Compartments Labeled with pH-VSR Represent a Complex Population with Variable pH

When pH of the population of pH-VSR compartments was analyzed more closely, a broader distribution of pH values, compared with ST-pH, in both tobacco (Figure 4A) and *Arabidopsis* (see Supplemental Figure 5 online) was observed. We reasoned that the pH heterogeneity within pH-VSR compartments might have functional significance. Since VSR compartments have different sizes, we asked whether compartment size and pH were related (see Supplemental Figure 6 online). Analysis of VSR particle size revealed an apparent bimodal distribution, yet no correlation between particle size and pH was found (see Supplemental Figure 6 online). Previous work indicated that VSRs are mostly colocalized with the target SNAP (Soluble NSF Attachment Protein) Receptor At-SYP21, a marker of PVCs, but that a small population also colocalized with Golgi (Li et al., 2002). Consequently, we examined the relationship between the pH of VSR compartments and their proximity to the *trans*-Golgi marker ST. As shown in Figure 4B, VSR compartments were mainly distinct from the *trans*-Golgi. Since it was previously suggested that endomembrane compartments can undergo

Table 1. List of Genetically Encoded Ratiometric pH-Sensitive Constructs Used in This Study

| Subcellular Compartment	pH Sensor Description	Construct Name
Cytoplasm; nucleus	pHluorin	Cyto-pH
ER	Tobacco chitinase SP, pHluorin, HDEL (1)	pH-HDEL
trans-Golgi	Sialyltransferase, pHluorin (2 and 3)	ST-pH
TGN and early endosomes	At-VSR2;1 SP, pHluorin, At-VSR2;1-YA (4 to 7)	pH-VSR-Y
Prevacuole and TGN	At-VSR2;1 SP, pHluorin, At-VSR2:1 (5 and 8 to 10)	pH-VSR
Late prevacuole	At-VSR2;1 SP, pHluorin, At-VSR2:1-IMAA (5)	pH-VSR-IM
Acidic/lytic vacuole and late prevacuole	Petunia (*Petunia hybrida*) aleurain SP, vacuolar sorting determinant of petunia aleurain, pHluorin (11 and 12)	Aleu-pH

References in the second column are as follows: 1, Gomord et al. (1997); 2, Wee et al. (1998); 3, Boevink et al. (1998); 4, daSilva et al. (2006); 5, Saint-Jean et al. (2010); 6, Foresti et al. (2010); 7, Drakakaki et al. (2006); 8, Paris et al. (1997); 9, Ahmed et al. (1997); 10, Li et al. (2002); 11, Di Sansebastiano et al. (2001); 12, Humair et al. (2001).

maturation events (Scheuring et al., 2011), we analyzed in more detail the distance between VSR and ST compartments (Figures 4C and 4D) and their pH. The distribution of individual VSR compartments indicated that only 2% colocalized with ST bodies, while 28% were associated, and the remaining 70% showed little to no colocalization (Figure 4E). These results fit well with previously published VSR localization data obtained using fluorescence as well as electron microscopy (Ahmed et al., 1997; Paris et al., 1997; Li et al., 2002). Surprisingly, we found no obvious relationship between pH and the distance between VSR organelles and the *trans*-Golgi. The pH of organelles associated with the *trans*-Golgi was identical (average pH 6.6) to the pH of VSR bodies that were distinct from Golgi (Figure 4D). These results indicated that the distance from the *trans*-Golgi is not a good criterion to distinguish between different populations of VSR organelles.

The pH in the Lumen of the TGN Is More Acidic Than That in the PVC and the Late PVC

In order to further analyze the pH distribution of the population of VSR organelles, we coexpressed pH-VSR with RFP-SYP61 to
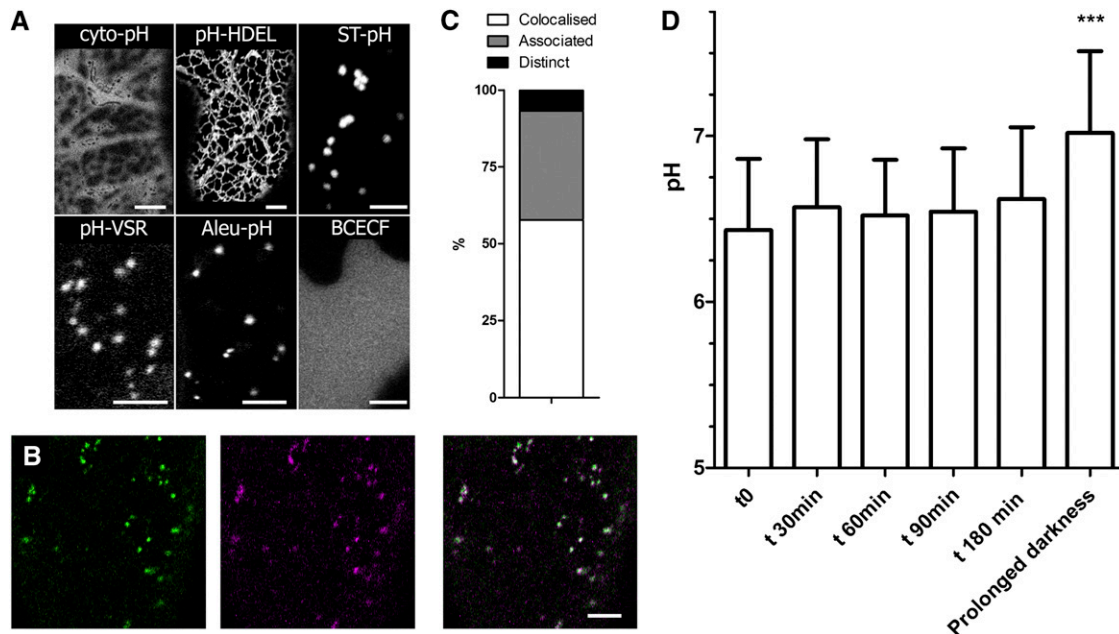
Figure 2. Subcellular Localization Pattern of pH Sensors Expressed in Tobacco Epidermal Cells.

(A) Representative expression pattern of tobacco epidermal cells transiently expressing pHluorin sensors or loaded with the dye BCECF-AM (vacuole).
(B) Colocalization of pH-VSR (green) with Tag-RFP-VSR (magenta) in transiently cotransformed tobacco epidermal cells.
(C) Percentage of Tag-RFP-VSR compartments that are colocalized with pH-VSR–containing compartments.
(D) pH in pH-VSR compartments measured in plants maintained in darkness.
Bars = 5 µm. Error bars are SD; *n* > 128. The pH measured at extended darkness significantly differed from the other values, Tukey test, ***P value < 0.001.
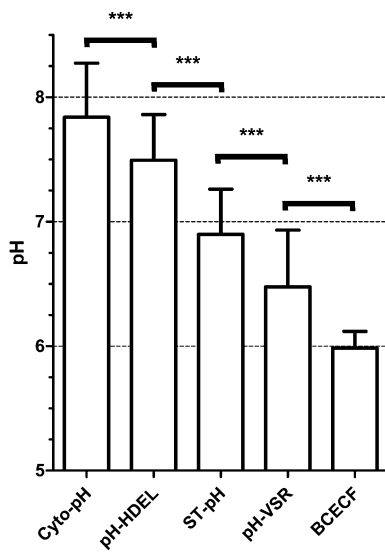
Figure 3. Luminal pH of Different Endomembrane Compartments.

Measurement of pH was performed in tobacco epidermal cells transiently expressing the pHluorin sensors (Cyto-pH for cytoplasm, pH-HDEL for ER, ST-pH for *trans*-Golgi apparatus, and pH-VSR for TGN and PVC compartments) or the dye BCECF-AM for the vacuole. $n > 150$, Tukey test, ***P value < 0.001; error bars are SD.

identify the TGN (Foresti et al., 2010). As shown in Figures 5A and 5B, VSR organelles segregated into three subpopulations that either colocalized with the TGN (23%), were associated (22%), or were physically distinct (55%). Interestingly, the pH appears to gradually increase with distance away from the TGN (Figure 5C). As shown in Figure 5D, the average luminal pH measured by the TGN-localized VSR was pH 6.1. The luminal pH of VSR compartments that are closely associated with the TGN was 6.4, while the population of VSR bodies that are distinct from the TGN had a luminal pH significantly more alkaline (pH 6.8). These results suggest that the pH within the TGN ($pH_{TGN} = 6.1$) is more acidic than that in the PVC (i.e., distinct from TGN, $pH_{PVC} = 6.7$). In a complementary approach, we coexpressed pH-VSR with Rha1, a late PVC marker (Lee et al., 2004; Foresti et al., 2010). We chose Rha1 because, in contrast with PEP12 (Foresti et al., 2006) or Ara7 (Kotzer et al., 2004), it has not been reported to affect VSR distribution when expressed at low levels in cells (Bottanelli et al., 2012). As shown in Figures 5E to 5G, we observed that almost all VSR compartments were distinct from late PVC (75%). Unlike what was measured with the SYP61-TGN marker, VSR compartments that were associated with the late PVC were more alkaline (Figure 5H). Importantly, we found that coexpression of the markers SYP61 and Rha1 did not affect the average pH in the lumen of VSR compartments.

In order to better understand the significance of our pH measurements to intracellular trafficking, we generated and expressed previously described trafficking mutants of the VSR receptor with pHluorin (Saint-Jean et al., 2010). The mutation of Y to A in the motif YXXΦ (pH-VSR-Y) prevents VSR from entering the anterograde route toward the vacuole and leads to

default transport to the plasma membrane. The fusion pH-VSR-IM carries the double mutation IM to AA that prevents recycling from the PVC. As a result, pH-VSR-Y is expected to label the earliest VSR compartments of the anterograde route as well as possible recycling endosomes, while pH-VSR-IM is expected to transiently label the last compartments prior to fusion with the vacuole, namely, late PVC. Colocalization with SYP61 indicated that, as expected, pH-VSR-Y was more often colocalized or associated with the TGN than its nonmutated pH-VSR equivalent (72% instead of 45%; Figures 6A and 6B compared with Figure 5B). Conversely, 75% of pH-VSR-IM particles colocalized with Rha1-mcherry and only 17% were distinct from the late PVC (Figures 6E and 6F), thus confirming that the IM mutation prevented VSR recycling. Most importantly, the pH of the TGN and possible recycling endosomes labeled by pH-VSR-Y was 6.5 and was significantly more acidic than the pH of the late PVC labeled by pH-VSR-IM (pH 7.1; analysis of variance [ANOVA], P value = 2.9E-8) (Figures 6C, 6D, 6G, and 6H). These results suggest that the TGN is more acidic than the PVC and the late PVC.

Given this surprisingly high pH of the late PVC, we also used a soluble pH sensor, Aleu-pH, to obtain complementary measurements. In contrast with VSR, Aleu-pH does not recycle and is detected transiently in the late PVC after 2 d of expression, and prior to reaching the vacuole. As expected, we found that 62% of Aleu-labeled organelles were colocalized with the late PVC marker Rha1 (see Supplemental Figure 7 online). Surprisingly, even if the pH in the late PVC measured with Aleu-pH (pH 6.5) remained significantly more alkaline than that in the TGN (ANOVA, P value = 3.56 E-5), it was lower than the pH measured using pH-VSR-IM, 7.1 (ANOVA, P value = 2.9 E-5). In order to check the orientation of the pH-VSR-IM fusion protein, we performed a proteinase K digestion on microsomes from transiently transformed tobacco leaves (see Supplemental Figure 8 online). It was shown previously that VSR is a type I membrane protein with a small C-terminal domain facing the cytosol (Kirsch et al., 1994). We used a combination of two antibodies, one recognizing pHluorin that is predicted to be luminal and one specific for the C terminus of VSR cytosolic domain (see Supplemental Figure 8A online). We found that pH-VSR-IM was oriented like the native tobacco VSR and two control VSR fusions, since we detected a digested form (d) at 110 kD that was 5 kD smaller than the undigested fusion protein (u); most importantly, this digested band was detected only with the antibody specific for the luminal domain, namely, the anti-GFP/pHluorin (see Supplemental Figure 8A online). This result indicates that the topology of pH-VSR-IM was as expected and that the pH measurement likely represents the lumen of the late PVC.

To summarize, using several independent approaches, we systematically identified an alkalinization of pH from the TGN, pH 6.1, to the late prevacuole, pH 7.1 (Figure 7). This alkalinization appears to be gradual, as shown in Figures 5C and 5G, suggesting some maturation events occur within the VSR organelles. The pH in the PVC, represented by the fraction of VSR organelles that was distinct from the TGN, was intermediate, pH 6.7 (Figure 7). All three pH values were significantly different from each other (Tukey test, P value < 0.001).
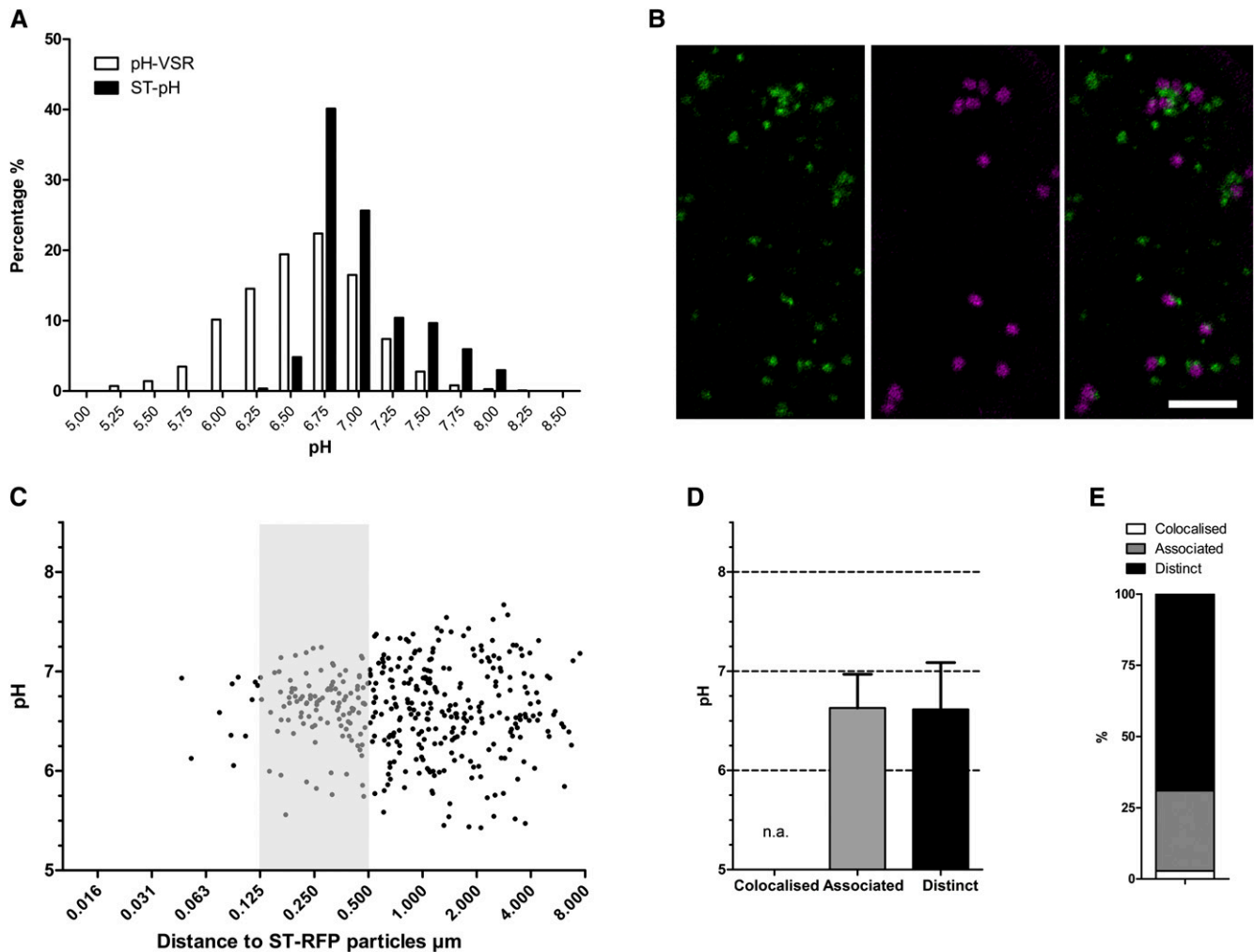
Figure 4. The pH of VSR Compartments Does Not Correlate with Distance from the *trans*-Golgi in Tobacco Epidermal Cells.

(A) Distribution of pH values of VSR (white) and *trans*-Golgi (black) compartments.

(B) Colocalization of pH-VSR (green) with ST-RFP (magenta) in transiently cotransformed tobacco epidermal cells. Bar = 5 μm.

(C) The average pH in pH-VSR compartments as a function of their distance from the closest *trans*-Golgi compartment labeled with ST-RFP. Three populations are identified: colocalized (< 125 nm), associated (shaded area between 125 and 500 nm), or distinct (above 500 nm); *n* = 386.

(D) Average pH in three populations of VSR compartments that are either associated or distinct from ST-RFP. n.a., not applicable.

(E) Proportion of pH-VSR particles belonging to three localization classes (*n* = 386).

ANOVA test. No significant difference between pH in associated and distinct VSR organelles. Distance is expressed in logarithmic scale. Error bars are SD.

pH Homeostasis in the TGN and PVC Is Regulated by Endosomal V-ATPase and NHX Antiporter and Is Required for Vacuolar Trafficking

Next, we probed the mechanisms involved in establishing the pH in VSR organelles. The V-ATPase subunit VHAa1 is localized to the EE/TGN and is believed to play a central role in the acidification of the secretory pathway (Dettmer et al., 2006). Indeed, we found that 39% of pH-VSR compartments colocalized with VHAa1-RFP (Figures 8A and 8B). As found previously, the EE/TGN fraction of VSR organelles was more acidic than the PVC (Figure 8E; Tukey test, P value < 0.001). Recently, it was proposed that endosomal NHX antiporters are also

necessary for regulating endosomal pH and required for proper vacuolar sorting (Bassil et al., 2011b, 2012). Consequently, we coexpressed pH-VSR with NHX5-RFP and found that 23% of pH-VSR colocalized with NHX5-RFP (Figures 8C and 8D). We expect that NHX5 antiport activity contributes to the alkalinization of the TGN. Indeed, the population of VSR organelles containing NHX5 was significantly more alkaline than those VSR compartments devoid of NHX5 (Figure 8F; Tukey test, P value < 0.001). Coexpression of neither VHAa1 nor NXH5 affected the average pH in VSR compartments. A comparison of the two coexpression experiments (Figure 8G) indicated that the pH of VSR compartments containing VHAa1 was significantly more acidic (pH 6.2) than that of those VSR organelles containing
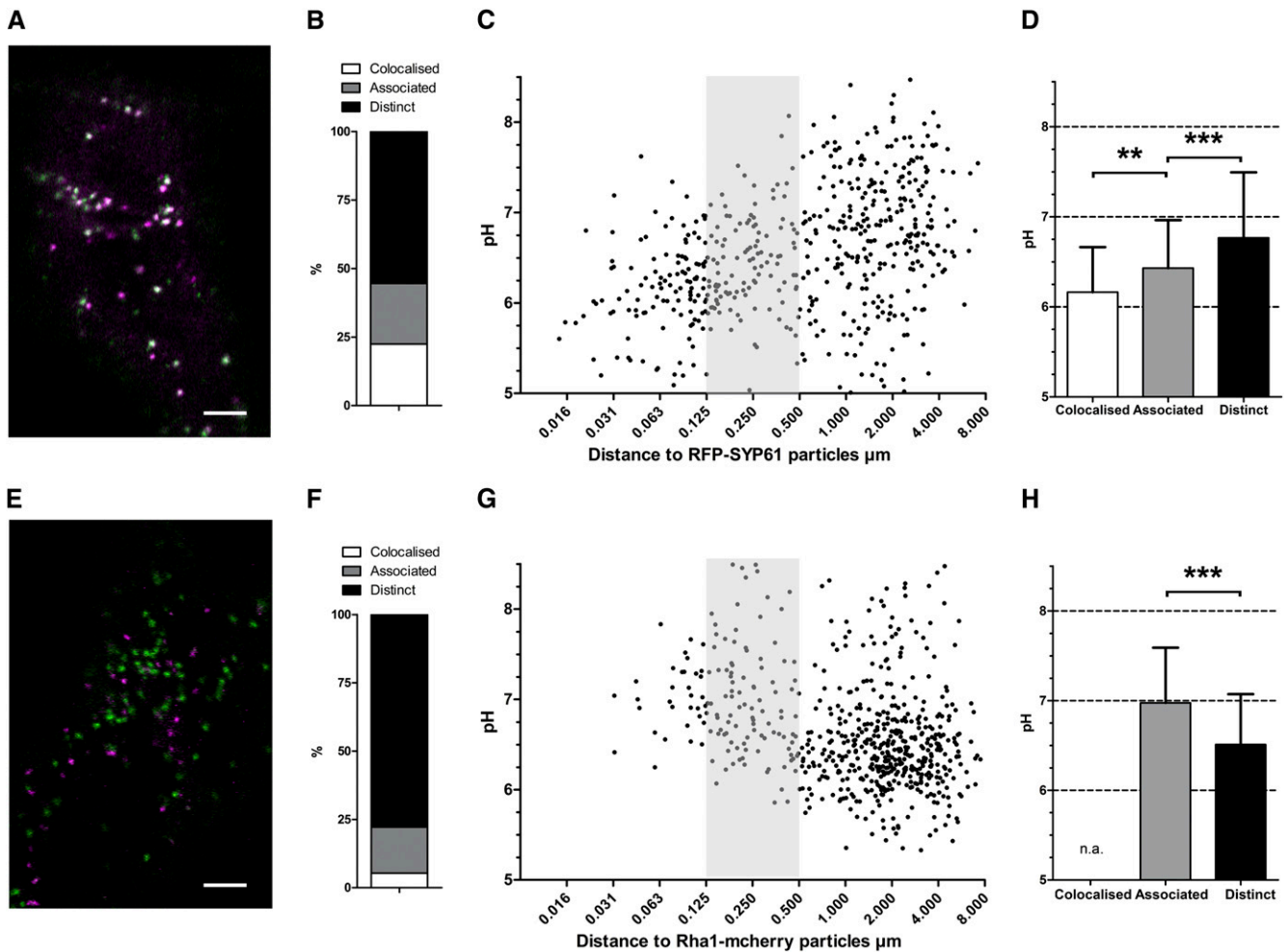
Figure 5. The TGN Subpopulation of VSR Compartments Is More Acidic Than the VSR Structures Associated with the Late PVC in Tobacco Epidermal Cells.

Coexpression of pH-VSR with RFP-SYP61 (**[A]** to **[D]**) or Rha1-mCherry (**[E]** to **[H]**).

(A) and **(E)** Confocal images showing the coexpression of pH-VSR (green) with either RFP-SYP61 (**[A]**, magenta) or Rha1-mCherry (**[E]**, magenta).

(B) and **(F)** Percentage of pH-VSR compartments that are colocalized with either RFP-SYP61 **(B)** or Rha1-mCherry compartments **(F)**.

(C) and **(G)** Average pH of pH-VSR compartments as a function of their distance from the closest TGN body labeled with RFP-SYP61 **(C)** or the closest late PVC body labeled with Rha1-mCherry **(G)**. Three populations are identified: colocalized (<125 nm), associated (shaded area between 125 and 500 nm), or distinct (above 500 nm).

(D) and **(H)** Average pH found in the three populations of organelles that were colocalized with (white), associated with (gray), or distinct from (black) RFP-SYP61 **(D)** or Rha1-mCherry **(H)**.

$n > 118$, Tukey test, **P value<0.01 and ***P value < 0.001. Distance is expressed in logarithmic scale. n.a., not applicable. Error bars are SD. Bars = 5 μm.

NHX5 (pH 6.4; ANOVA, P value = 0.008). We noted that this difference was not as steep as the one previously measured between the TGN and PVC (Figure 7). This can be explained by the fact that VHAa1 and NHX strongly colocalized in both *Arabidopsis* (Bassil et al., 2011b) and tobacco epidermal cells (see Supplemental Figure 9A online). Given this strong colocalization, we assumed that if the amount of VHAa1 and NHX varied within a given population of VSR compartments, it would affect luminal pH. To address this hypothesis, we analyzed cells coexpressing NHX6-YFP with VHAa1-RFP and found that, indeed, the relative fluorescence of the two markers

varied between organelles (see Supplemental Figure 9A online, plots 1 and 2).

In order to assess the role of pH in vacuolar transport, we used a set of drugs known to interfere with vacuolar trafficking. As shown in Figure 9A, all treatments significantly modified the pH in VSR organelles compared with controls (Tukey test, P value < 0.001). Wortmannin, latrunculin B, and concanamycin A led to the alkalinization of VSR compartments with the strongest effects observed with concanamycin A, a drug known to specifically inhibit the V-ATPase and interfere with the transport of soluble vacuolar proteins by acting at a step prior to reaching
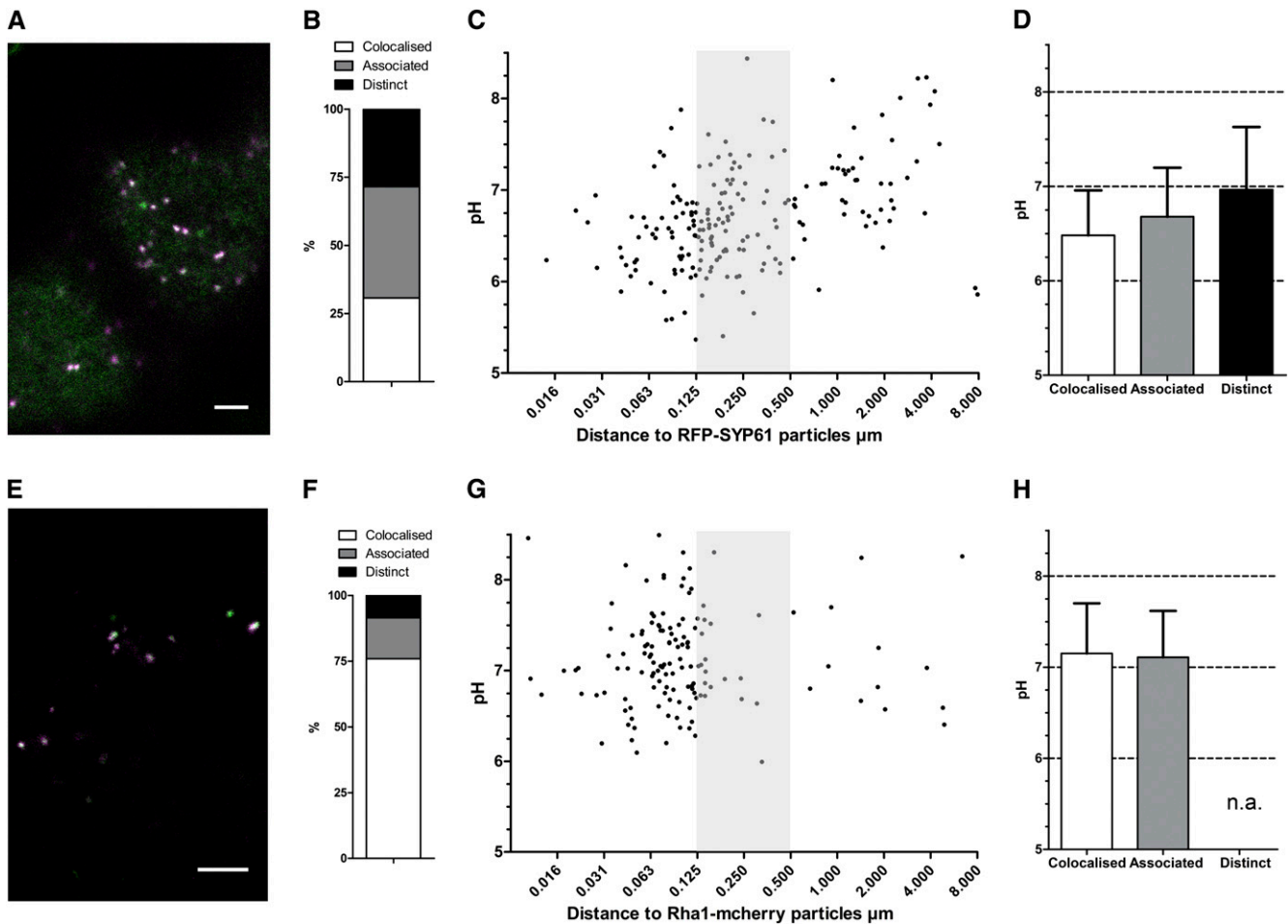
Figure 6. The Acidic-to-Alkaline Gradient Is Related to Anterograde Trafficking of VSR from TGN to Late PVC in Tobacco Epidermal Cells.

Coexpression of pH-VSR-Y with RFP-SYP61 (**[A]** to **[D]**) and pH-VSR-IM with Rha1-mCherry (**[E]** to **[H]**).

(A) and **(E)** Confocal images showing the coexpression of pH-VSR sensors (green) and either RFP-SYP61 (**[A]**, magenta) or Rha1-mCherry (**[E]**, magenta).

(B) and **(F)** Proportion of pHluorin-labeled structures that colocalized either with RFP-SYP61 **(B)** or Rha1-mCherry **(F)**.

(C) and **(G)** Average pH in compartments labeled with either pH-VSR-Y **(C)** or pH-VSR-IM **(G)** as a function of their distance either from the closest TGN labeled with RFP-SYP61 **(C)** or from the closest late PVC labeled with Rha1-mCherry **(F)**. The pH of the three identified populations, colocalized (<125 nm), associated (shaded area between 125 and 500nm), or distinct (above 500 nm), are indicated in **(D)** and **(H)**.

Distance is expressed in logarithmic scale. n.a., not applicable. Error bars are SD. $n = 205$ in **(B)** to **(D)**; $n = 138$ in **(F)** to **(H)**. Tukey test, ***P value < 0.001. Bar = 5 μm.

the vacuole (Matsuoka et al., 1997). We tested the notion that antiporters alkalinize the lumen of VSR compartments using amiloride, an inhibitor of Na^+/H^+ antiporters (Blumwald and Poole, 1985). As shown in Figure 9A, amiloride leads to a significant acidification of VSR organelles. To confirm that these results were due to a direct effect of the drugs rather than an effect on protein localization, we determined whether VHAa1 (Figure 9B) or NHX5 (Figure 9C) was still present in the VSR compartments after treatment with the drugs and found that concanamycin A had almost no effect on the VSR/VHAa1 distribution (Figure 9B) and slightly increased the population of VSR with NHX5 (Figure 9C). Amiloride slightly increased the fraction of VSR organelles with VHAa1 and had no effect on the VSR-

NHX5 distribution. These results suggested that the pH changes observed upon treatment with concanamycin A or amiloride were most likely due to the respective inhibition of V-ATPase or NHX activity. This supports the idea that pH homeostasis in VSR compartments is maintained by both V-ATPase and NHX, likely regulating pH in an opposing manner, with V-ATPase acidifying and NHXs alkalinizing endosomes. If this were the case, then the concomitant use of both concanamycin and amiloride should result in an intermediate pH, compared with when either was used alone. Results indicated in Figure 9A are consistent with this notion. Wortmannin and latrunculin B also increased the luminal pH of VSR compartments, suggesting that the balance between V-ATPases and NHX might be altered. Indeed,
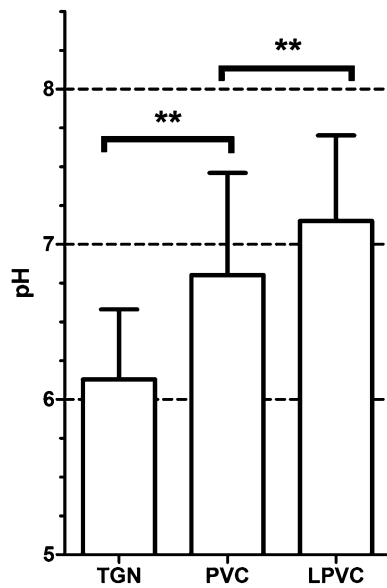
Figure 7. Average Luminal pH of Compartments between the Golgi and Vacuole in Tobacco Epidermal Cells.

The average pH values were obtained from the subpopulations of pH-VSR colocalized with SYP61-RFP (TGN), pH-VSR associated or distinct from SYP61-RFP (PVC), or pH-VSR-IM colocalized with Rha1-mcherry (late PVC [LPVC]). pH measurements from 120 TGN, 412 PVC, and 105 late PVC distinct organelles. Tukey test, **P value < 0.01. Error bars are SD; *n* > 63.

treatment with wortmannin did significantly induce a separation of VHAa1 and VSR structures (Figure 9B; see Supplemental Figure 10A online) and also tripled the number of NHX5-positive VSR compartments (Figure 9C; see Supplemental Figure 10B online). Latrunculin B slightly increased the fraction of VSR that colocalized with VHAa1 and had no effect on the colocalization of VSR with NHX5 (Figures 9B and 9C). The increase in VSR and VHAa1 colocalization as well as the observed increase in pH of VSR compartments following latrunculin B treatment suggests that V-ATPase activity requires association with actin filaments.

DISCUSSION

pH of the Plant Endomembrane System

In this study, we developed pH sensors, targeted them to specific cellular compartments, and used live-cell imaging to measure the luminal pH along the plant secretory pathway. Similar to reports in animal cells (Llopis et al., 1998; Miesenböck et al., 1998), plant cells displayed a gradual acidification from the ER to the lysosome/vacuole, as summarized in Figure 10. The pH was ~1.5 pH units more acidic in the vacuole compared with the ER in tobacco cells, and the difference was nearly 2 pH units in *Arabidopsis* cells.

Overall, the pH values obtained in plant intracellular compartments are similar but slightly more alkaline than their animal cell equivalents (Paroutis et al., 2004). The pH reported in

lysosomes (pH 5.5) is also similar to the pH we obtained in vacuoles of tobacco epidermal cells (pH 6) and in *Arabidopsis* root tip cells (pH 5.5) as well as to earlier published results (Krebs et al., 2010; Bassil et al., 2011b). The TGN/EE was significantly more acidic (0.5 pH units) than the *trans*-Golgi, as observed in mammalian cells (Llopis et al., 1998). One intriguing result that we found was that the pH of the TGN was more acidic than that of the PVC and of the late PVC (discussed further below).

We obtained very similar pH values in the TGN subpopulation of VSR compartments that colocalized with SYP61 or VHAa1 (pH 6.1 and 6.2, respectively). In plants, VHAa1 and SYP61 strongly overlap, with VHAa1 being more distant to the Golgi compared with SYP61 (Kang et al., 2011). Curiously, while the colocalization of VSR to both TGN markers clearly identified a pH gradient with the distance from the TGN, the same experiment using the *trans*-Golgi marker ST failed to identify any pH variation within VSR organelles. These results may indicate that the acidic population of VSR could represent mainly the "free" subpopulation of TGN with a Golgi-independent dynamic (Viotti et al., 2010). Collectively, our results highlight the dynamic nature of compartments and emphasize the limitations of using fixed tissue that merely captures a snapshot in time and cannot inform on either the origin or destination of particular organelles.

The identification of subpopulations of VSR organelles with distinct luminal pH values suggests that pH and trafficking are intimately connected. In plants, the TGN and early endosome are both labeled by VHAa1 (Dettmer et al., 2006). In animal cells, the early endosome is more alkaline than the TGN, and the pH of TGN obtained in this study is closer to the animal TGN pH (pH 5.9) than that of animal early endosomes (pH 6.3). In our hands, only a fraction of VHAa1 and SYP61 organelles colocalized with VSR, and it is possible that the pH_{TGN} measured with VSR represents only a subpopulation of all TGN/EE compartments, at least in tobacco. Interestingly, the pH in the SYP61 fraction of pH-VSR-Y compartments (pH = 6.5) was significantly more alkaline than that measured with pH-VSR (6.1, P value < 0.0001). It was previously shown that VSR can cycle through the plasma membrane and that mutating the YMPL motif would force VSR into this alternative pathway (daSilva et al., 2006; Saint-Jean et al., 2010). It is therefore tempting to conclude that the SYP61 fraction labeled with pH-VSR-Y also includes early and recycling endosomes.

To analyze later compartments in the vacuolar route, we used the well-characterized marker Rha1, a GTPase that localizes to late endosome/MVB/late PVC and functions in trafficking to the vacuole (Nielsen et al., 2008; Geldner et al., 2009; Foresti et al., 2010). As shown previously, we found that VSR does not localize to the late PVC, supporting the notion that VSR recycles from the PVC before it can reach the late PVE (daSilva et al., 2005; Saint-Jean et al., 2010), giving rise to a late PVC that is depleted of receptors (Foresti et al., 2010) and enriched in vacuolar proteins and rab5 GTPases (Bottanelli et al., 2012). Almost a fourth of the compartments labeled with pH-VSR were closely associated with the late PVC and may represent VSR organelles previously identified, using electron microscopy, to be in close periphery of MVBs (Otegui et al., 2006; Viotti et al., 2010; Scheuring et al., 2011) or of functionally similar
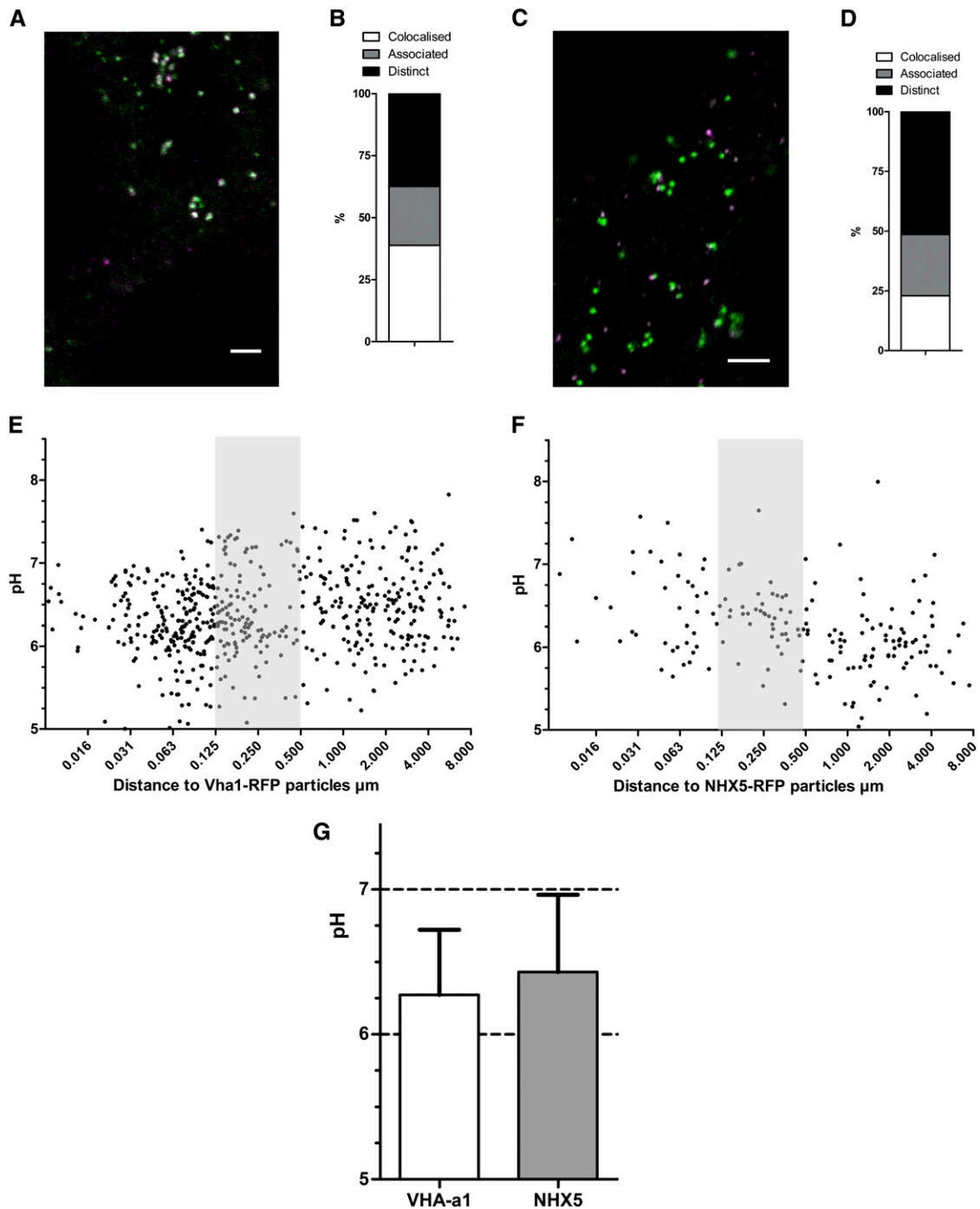
Figure 8. The Population of VSR Compartments Colocalizing with VHAa1 Is More Acidic Than the Population Colocalizing with NHX5 in Tobacco Epidermal Cells.

Coexpression of pH-VSR with VHAa1-RFP (**[A]**, **[B]**, and **[E]**) or NHX5-RFP (**[C]**, **[D]**, and **[F]**).

(A) and **(C)** Confocal images with pH-VSR (green) and VHAa1-RFP **(A)** or NHX5-RFP **(C)** in magenta.

(B) and **(D)** Percentage of pHluorin-labeled structures that colocalized with (white), associated with (gray), or were distinct from (black) either VHAa1-RFP **(B)** or NHX5-RFP **(D)**.

(E) and **(F)** Average pH in independent compartments labeled with pH-VSR as function of their distance either from the closest TGN labeled with VHAa1-RFP **(E)** or the closest compartment labeled with NHX5-RFP **(F)**. Three populations are identified: colocalized (<125 nm), associated (gray zone between 125 and 500 nm), or distinct (above 500 nm).

(G) Average pH found in pH-VSR structures colocalized with VHAa1-RFP or NHX5-RFP.

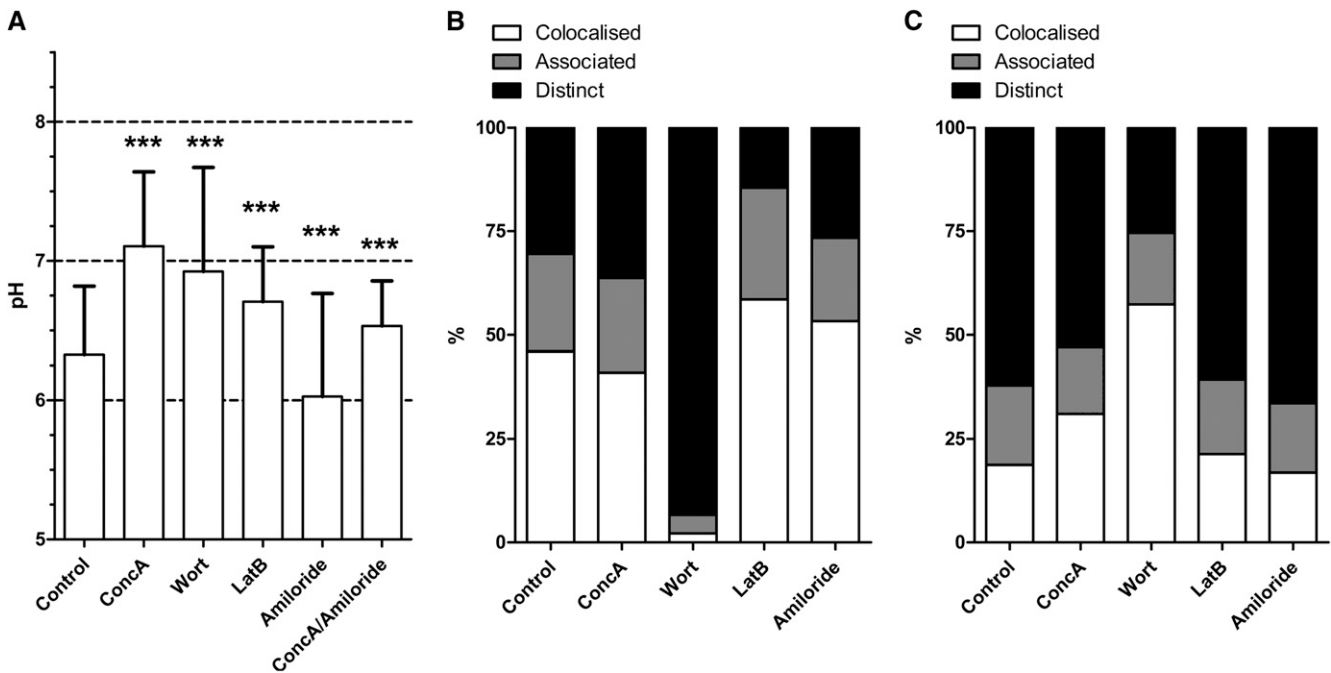$n > 183$. Tukey test, P value < 0.05. Distance is expressed in a logarithmic scale. Error bars are SD. Bars = 5 μm.

Figure 9. Inhibitors of Vacuolar Transport Alter the pH of VSR Compartments.

Tobacco epidermal cells expressing pH-VSR were treated with 1 µM concanamycin A (ConcA) for 60 min, 10 µM wortmannin (Wort) for 60 min, 25 µM latrunculin B (LatB) for 60 min, or 200 µM amiloride for 60 min, alone or in combination with concanamycin A. Tukey test compared with control; ***P value < 0.001. Error bars are SD.

(A) Average pH found in VSR particles after treatment compared with noninfiltrated controls.

(B) and **(C)** Distribution of pH-VSR compartments that colocalized with VHAa1-RFP **(B)** or NHX5-RFP **(C)** following drug treatments.

compartments probably in the process of fusing to the central vacuole (Paris et al., 1997). Interestingly, the late PVC–associated compartments were significantly more alkaline than the rest of the VSR organelles (P value < 0.0001). Since pH-VSR is not degraded, it is tempting to postulate that these alkaline compartments are VSR recycling structures.

To measure the luminal pH of the late PVC, we chose to fuse pHluorin with aleurain (Aleu-pH) or a mutated form of pH-VSR that fails to recycle from the PVC (Saint-Jean et al., 2010). Surprisingly, although these two fusions both colocalized with the late PVC marker Rha1, the pH values obtained were different: 6.5 for the Aleu-pH and 7.1 for pH-VSR-IM. This discrepancy might be due to the fact that Aleu-pH is soluble, while pH-VSR-IM is membrane bound and, therefore, the two sensors might have altered pK_a's due to these different microenvironments.

Maintenance of Organelle pH Homeostasis

The observation that the TGN is more acidic than the late PVC was unexpected primarily because the pH gradient opposes the gradual acidification of compartments from the ER and the vacuole that was measured. The activity of endosomal V-ATPase is essential to maintain the acidity of the VSR organelles, as indicated by the finding that application of concanamycin A led to alkalinization of VSR organelles with no change in VHAa1/

VSR colocalization. Electron microscopy studies showed that the identity and independence of the TGN is significantly affected by concanamycin A. As a result, VHAa1, SYP61, and VSR are redistributed toward the Golgi (Viotti et al., 2010; Scheuring et al., 2011), suggesting a loss of differentiation beyond the *trans*-Golgi. Wortmannin treatment also strongly modified the pH in VSR compartments, but in this case, it was due to an exclusion of VHAa1. The same treatments lead to an opposite effect in VSR structures containing NHX5, suggesting that not only the proper distribution of V-ATPase, but also that of NHX5/6 in VSR compartments, are essential to maintain the luminal pH difference between the TGN and the late PVC. The acidification of VSR compartments by amiloride adds strength to this argument.

Our results support the notion that the activity of V-ATPase is necessary for the acidification of VSR structures and consequently for vacuolar transport. These results fit well with the observation that VHAa1 is mainly concentrated in the TGN/EE but cannot be detected in the late endosome (Dettmer et al., 2006). Other H⁺ pumps, such as H⁺-pyrophosphatase, have not yet been identified in endosomal compartments (Robinson et al., 2012). In addition to luminal acidification, our results also suggest that organelle alkalinization, likely to be mediated at least in part by NHX-type endosomal antiporters, such as NHX5 and NHX6 in *Arabidopsis*, is required for the regulation of luminal pH homeostasis. These results are in accordance with the proton
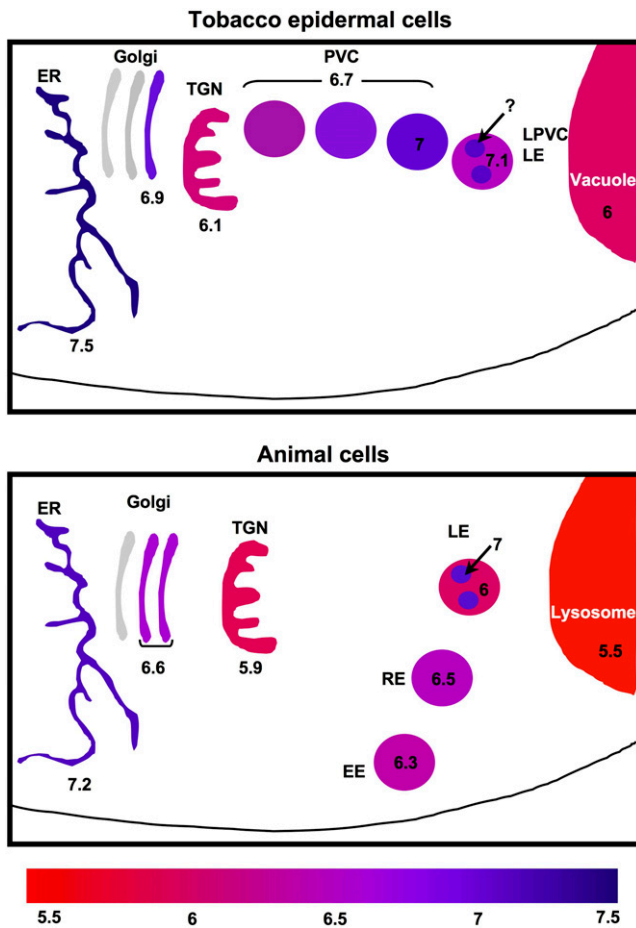
Figure 10. A Model Comparing the Steady State pH of Compartments in the Secretory Pathway of Tobacco Epidermal Cells and Animal Cells.

Colors of the lumen correspond to the steady state pH in plant intracellular compartments and marked with the approximate pH measured in this study. RE, recycling endosome; EE, early endosome; LE, late endosome; LPVC, late prevacuolar compartment.

leak model (Demaurex, 2002; Bassil et al., 2012) and with the fact that the double knockout mutant *nhx5 nhx6* is impaired in soluble protein trafficking to the vacuole (Bassil et al., 2011b). Direct measurement of endosomal pH in *nhx5 nhx6* knockouts or V-ATPase knockdowns would address this hypothesis more directly, assuming that the ability to target pH sensors would not be impaired by altered pH in knockouts.

Binding and pH

A clear link between pH in VSR bodies and transport to the vacuole is possible because the application of drugs known to affect vacuolar transport, such as concanamycin A, amiloride, and wortmannin, also significantly affect compartmental pH. Our results suggest that vacuolar trafficking mediated by VSR occurs between an acidic TGN and a more alkaline late PVC. The current model for VSR-mediated transport of soluble proteins to the vacuole proposes that

binding occurs in the TGN and ligand release occurs in the PVC due to a decrease in pH. This model is based on several independent in vitro binding assays (Kirsch et al., 1994; Ahmed et al., 2000; Shimada et al., 2003a) and resembles that of the mannose-6-phosphate receptor in mammalian cells (Kornfeld, 1992). In these assays, binding was performed on affinity columns harboring various vacuolar sorting determinants with a membrane fraction containing the receptor. The binding step itself was performed at pH 7.0, and release was obtained by eluting with a solution at pH 4. One in vitro binding assay of VSR to its ligand has been performed to quantify binding as a function of pH, using the competition between iodinated and an unlabeled aleurain vacuolar targeting sequence. This binding curve is bell-shaped with optimal binding occurring at pH 6.2 (Kirsch et al., 1994). Below, but most importantly also beyond this optimum, binding decreased significantly, being 20% less efficient at pH 7.0 than the optimum at pH 6.2. Interestingly, the in vivo luminal pH value of 6.1 that we measured in the TGN of tobacco epidermal cells is very close to the optimal in vitro binding pH. We found further significant alkalinization of pH between PVC and late PVC, suggesting that if pH-mediated release occurs in plants, it might be at a step between the TGN and PVC and caused by alkalinization rather than acidification. The KDEL recycling receptor ERD2 also displays a bell-shaped in vitro pH binding curve (Wilson et al., 1993), and the difference in binding efficiency is 18% between the known pH 6.7 in *cis*-Golgi where binding of ERD2 occurs, and receptor release at pH 7.2 in the ER. Similarly, a 20% decrease in binding affinity of VSR to its ligand due to alkalinization could theoretically explain the release of the ligand in vivo. Nevertheless, in vitro binding assays cannot accurately reflect what might occur in vivo where many factors could affect VSR binding to its ligands, such as VSR homodimerization (Kim et al., 2010) or the ionic environment of organelles. VSR contains three epidermal growth factor repeats that play a role in modulating its binding to the ligand (Herz et al., 1988; Rogers et al., 2004). Indeed, it was shown that at least some of the seven members of the VSR family in *Arabidopsis* exhibit Ca^{2+}-dependent binding to ligands (Watanabe et al., 2002, 2004). It was recently shown that the concentration of Ca^{2+} in Golgi is ~0.7 μM (Ordenes et al., 2012), much lower than that in the ER where Ca^{2+} concentrations are in the mM range.

In conclusion, we measured the pH in the lumen of intracellular compartments of the endomembrane system in plants. Using a vacuolar receptor to target the sensor to intermediate compartments between the Golgi and vacuole, we also identified the existence of a complex population of organelles and of luminal pH tuning which is likely to be critical in transport of soluble proteins to the vacuole. Future experiments should further analyze changes in pH together with dynamic trafficking processes in order to correlate pH with organelle maturation, as proposed recently for the TGN/EE (Scheuring et al., 2011), and pH homeostasis. It would also be interesting to assess receptor ligand binding in vivo, particularly since the pH reported here for the TGN and late PVC is contrary to what was predicted from in vitro studies.

METHODS

Constructs

We used pHluorin (Bagar et al., 2009) to generate several genetically en- coded pH sensors and target to specific intracellular compartments (see Table 1 for the list and Supplemental Table 1 online). To target the sensor to the ER lumen, the signal peptide from tobacco (*Nicotiana tabacum*) chiti- nase (Di Sansebastiano et al., 1998) and the tetrapeptide HDEL (Gomord et al., 1997) was used. To label *trans*-Golgi, we used part of the mammalian sialyl transferase as described previously (Boevink et al., 1998; Wee et al., 1998). The fusion of pHluorin at this position results in the luminal locali- zation of the pH sensor. For VSR fusion proteins (see Supplemental Figure 11 for sequence details and Supplemental Table 1 online) the pHluorin coding sequence was placed between the signal peptide and the mature sequence of At-VSR2;1 (Saint-Jean et al., 2010) in which N terminus is luminal (Kirsch et al., 1994). Aleu-pH was made by fusion of the petunia (*Petunia hybrida*) aleurain signal peptide and vacuolar sorting signal (Humair et al., 2001) before the pHluorin coding sequence.

Transient and Stable Expression

For transient expression in leaves, 3- to 4-week-old tobacco (*N. tabacum* cv SR1) plants were infiltrated with *Agrobacterium tumefaciens* strain GV3101 p2260 as described previously (Sparkes et al., 2006). A small lesion to the leaves facilitated the transformation (infiltration solution $OD_{600} = 0.1$).

For colocalization studies, we used red fluorescent fusion constructs that were previously described: pVHAa1:genomicVHAa1-mRFP (Uemura et al., 2012), p35s:NHX5-mRFP (Bassil et al., 2011b), p35s:NHX6-YFP (Bassil et al., 2011b), p35s:ST-RFP (Saint-Jore et al., 2002), p35s:SYP61- mRFP (Foresti et al., 2010), and pUBQ10:Rha1-mcherry (Geldner et al., 2009).

Stable transformations of *Arabidopsis thaliana* ecotype Columbia-0 were performed according to the floral dip method (Clough and Bent, 1998).

Confocal Microscopy

We observed samples 48 to 72 h after transient expression in tobacco epidermal cells or from 4- to 5-day-old root tip cells of stably transformed *Arabidopsis*. Unless stated otherwise, tobacco plants were kept in 8-h:16-h light:dark cycles during transient expression. For pH measurements of pHluorin, images were taken on a LSM 510 META confocal microscope, set with sequential excitation at 405 nm/488 nm and single emission band-pass 505 to 530 nm. For colocalization experiments, a Zeiss LSM 780 confocal imaging system running in line-by-line sequential scanning mode was used, at 405-nm/488-nm excitation with a 505 to 530 photomultiplier (PMT) setting for pHluorin and at 561-nm excitation with a 585 to 610 PMT setting for all red fluorochromes.

Images were acquired with a ×63 PL-APO 1.4 oil objective with time integration of one frame per second. Theoretical *xy*- and *z*-axis resolutions were 70 and 160 nm (1 airy unit), respectively. Frame size of the image was 45 μm with a 16-bit color depth.

Images were processed using Adobe Photoshop F1 4.0 software.

pH Measurements

Recombinant pHluorin was produced in bacteria by induction with 1 mM isopropyl β-D-1-thiogalactopyranoside for 4 h. Bacteria were harvested and washed three times in water. The pellets were broken by sonication in phosphate buffer (10 mM Na_2HPO_4 and 2 mM KH_2PO_4). In situ cali- brations were performed for each individual confocal observation session. An aliquot of recombinant pHluorin was diluted in a series of buffers: MES-KOH or HEPES-KOH at different pH from 5 to 8.5. The ratio values were plotted as a function of pH, and a Boltzmann equation was used to fit sigmoidal curves with calibration data as described previously (Gao et al.,

2004; Schulte et al., 2006). The following equation was used (Graphpad Prism):

$$R = R_{min} + (R_{max} - R_{min})/\left(1 + exp^{(pKa-pH)}\right)$$

where *R* is the ratio value for a given pH, R_{min} and R_{max} designate the maximum and the minimum ratio obtained at either high or low pH, and pK_a designates pH value when half of the pHluorin is protonated.

Prior to data acquisition, we set the PMT offset with nontransformed plants to standardize the background. For each treatment, 10 to 20 cells were analyzed, and pH values were extrapolated out of the sigmoidal function obtained from in vitro calibration curves.

Colocalization Analysis

In order to quantify the extent of colocalization between compartments, we calculated the minimal distance between particle centroids using Velocity software (Perkin-Elmer). To confirm the method, we performed three experiments: (1) With 500-nm multicolor beads (TetraSpeck Fluorescent microsphere; Molecular Probes), we obtained a mean distance of 47 nm (see Supplemental Figure 2A online); (2) to analyze the degree of coloc- alization in vivo, we coexpressed the *trans*-Golgi marker ST fused with either pHluorin or RFP (see Supplemental Figure 2B online); and (3) to estimate the association of compartments, coexpression of the *cis*-Golgi marker ERD2- CFP with the *trans*-Golgi marker ST-RFP (see Supplemental Figure 2C online) was performed. We obtained average distances of 60 nm for compartment colocalization and 125 nm for associated compartments in vivo. Furthermore, given that the mean radius of the VSR compartment obtained electron microscopy studies was 450 nm, we set 500 nm as the maximum distance at which we can consider two organelles to be asso- ciated or maturing. We considered particles at a distance shorter than 125 nm to be colocalized, those between 125 and 500 nm to be associated (see Supplemental Figure 2 online, shaded areas), and those over 500 nm apart to be distinct. Quantification of colocalization data is expressed in per- centage of organelles, with 100% representing the total number of or- ganelles analyzed.

To relate pH with colocalization, individual organelles labeled with pHluorin were identified using Image J. The mean pH was then calculated for each organelle that was also analyzed for colocalization as described above.

Statistical Analysis

Measurements of pH were compared using ANOVA followed, when necessary, by a post hoc test (Tukey's Honestly Significant Difference) using the open-source statistical computing R software (Free Software Foundation; http://www.gnu.org/software/r/). For each condition, at least two biological replicates of 10 cells were used, which represent more than 100 individual compartments per condition. To allow robust sta- tistical analysis, we excluded pH measurements from any subpopulations of compartments representing <10% of the total number of labeled compartments.

Drug Treatments

Drug treatment was performed by infiltrating a piece of leaf for 60 min prior to observation. Latrunculin B was used at 25 μM (Calbiochem), wort- mannin at 10 μM (Sigma-Aldrich), concanamycin at 1 μM, and amiloride hydrochloride (Euromedex) at 200 μM.

Accession Numbers

Sequence data from this article can be found in the Arabidopsis Genome Initiative or GenBank/EMBL databases under the following accession

numbers: *VSR2.1*, At2g14720; *ERD2*, At1g29330; *NHX5*, At1g54370; *NHX6*, At1g79610; *Rha1*, At5g45130; *VHA-a1*, At2g28520; and *SYP61*, At1g28490.

Supplemental Data

The following materials are available in the online version of this article.

Supplemental Figure 1. Cellular Localization Pattern of pH Sensors and Corresponding pH Measurement in Stably Transformed *Arabidopsis thaliana* Root Tip Cells.

Supplemental Figure 2. Experimental Procedure to Distinguish between Colocalized and Associated Particles.

Supplemental Figure 3. Comparison of Vacuolar pH Measurements Using Either pHluorin or BCECF.

Supplemental Figure 4. Comparison of in vivo and in Situ pH Measurement Methods.

Supplemental Figure 5. pH Distribution in VSR Compartments and *trans*-Golgi in Stably Transformed *Arabidopsis* Root Tip Cells.

Supplemental Figure 6. The pH Distribution of VSR Compartments Is Not Correlated with the Size of Compartments.

Supplemental Figure 7. The luminal pH of Late PVC Organelles Measured by Aleu-pH Is Alkaline.

Supplemental Figure 8. The Fusion Protein pH-VSR-IM Has Its C Terminus Exposed in the Cytosol.

Supplemental Figure 9. The Relative Amount NHX and VHAa1 Varies from One Organelle to Another.

Supplemental Figure 10. Comparative Effect of Wortmannin on the Colocalization of VSR Compartments with Either VHAa1 or NHX5.

Supplemental Figure 11. Peptide Sequences of VSR-Based pH Sensors.

Supplemental Table 1. Constructs.

AUTHOR CONTRIBUTIONS

A.M., N.P., and E. Blumwald designed the research. A.M., N.P., E. Bassil, and C.A. performed research. E.J. contributed new analytic tools. A.M., N.P., E. Bassil, E. Blumwald, M.R., and H.S., wrote the article.

REFERENCES

Ahmed, S.U., Bar-Peled, M., and Raikhel, N.V. (1997). Cloning and subcellular location of an Arabidopsis receptor-like protein that shares common features with protein-sorting receptors of eukaryotic cells. Plant Physiol. **114:** 325–336.

Ahmed, S.U., Rojo, E., Kovaleva, V., Venkataraman, S., Dombrowski, J.E., Matsuoka, K., and Raikhel, N.V. (2000). The plant vacuolar sorting receptor AtELP is involved in transport of NH(2)-terminal propeptide-containing vacuolar proteins in *Arabidopsis thaliana*. J. Cell Biol. **149:** 1335–1344.

Bagar, T., Altenbach, K., Read, N.D., and Bencina, M. (2009). Live-cell imaging and measurement of intracellular pH in filamentous fungi using a genetically encoded ratiometric probe. Eukaryot. Cell **8:** 703–712.

Bassil, E., Coku, A., and Blumwald, E. (2012). Cellular ion homeostasis: Emerging roles of intracellular NHX Na$^+$/H$^+$ antiporters in plant growth and development. J. Exp. Bot. **63:** 5727–5740.

Bassil, E., Ohto, M.A., Esumi, T., Tajima, H., Zhu, Z., Cagnac, O., Belmonte, M., Peleg, Z., Yamaguchi, T., and Blumwald, E. (2011a). The *Arabidopsis* intracellular Na$^+$/H$^+$ antiporters NHX5 and NHX6 are endosome associated and necessary for plant growth and development. Plant Cell **23:** 224–239.

Bassil, E., Tajima, H., Liang, Y.-C., Ohto, M.-A., Ushijima, K., Nakano, R., Esumi, T., Coku, A., Belmonte, M., and Blumwald, E. (2011b). The Arabidopsis Na$^+$/H$^+$ Antiporters NHX1 and NHX2 control vacuolar pH and K$^+$ homeostasis to regulate growth, flower development, and reproduction. Plant Cell **23:** 3482–3497.

Blumwald, E., and Poole, R.J. (1985). Na$^+$/H$^+$ antiport in isolated tonoplast vesicles from storage tissue of *Beta vulgaris*. Plant Physiol. **78:** 163–167.

Boevink, P., Oparka, K., Santa Cruz, S., Martin, B., Betteridge, A., and Hawes, C. (1998). Stacks on tracks: the plant Golgi apparatus traffics on an actin/ER network. Plant J. **15:** 441–447.

Boss, W.F., Morré, D.J., and Mollenhauer, H.H. (1984). Monensin-induced swelling of Golgi apparatus cisternae mediated by a proton gradient. Eur. J. Cell Biol. **34:** 1–8.

Bottanelli, F., Gershlick, D.C., and Denecke, J. (2012). Evidence for sequential action of Rab5 and Rab7 GTPases in prevacuolar organelle partitioning. Traffic **13:** 338–354.

Brauer, D., Otto, J., and Tu, S.-I. (1995). Selective accumulation of fluorescent pH indicator, BCECF, in vacuoles of maize root-hair cells. J. Plant Physiol. **145:** 57–61.

Casey, J.R., Grinstein, S., and Orlowski, J. (2010). Sensors and regulators of intracellular pH. Nat. Rev. Mol. Cell Biol. **11:** 50–61.

Chanroj, S., Wang, G., Venema, K., Zhang, M.W., Delwiche, C.F., and Sze, H. (2012). Conserved and diversified gene families of monovalent cation/h(+) antiporters from algae to flowering plants. Front. Plant Sci. **3:** 25.

Clough, S.J., and Bent, A.F. (1998). Floral dip: a simplified method for Agrobacterium-mediated transformation of *Arabidopsis thaliana*. Plant J. **16:** 735–743.

daSilva, L.L., Foresti, O., and Denecke, J. (2006). Targeting of the plant vacuolar sorting receptor BP80 is dependent on multiple sorting signals in the cytosolic tail. Plant Cell **18:** 1477–1497.

daSilva, L.L., Taylor, J.P., Hadlington, J.L., Hanton, S.L., Snowden, C.J., Fox, S.J., Foresti, O., Brandizzi, F., and Denecke, J. (2005). Receptor salvage from the prevacuolar compartment is essential for efficient vacuolar protein targeting. Plant Cell **17:** 132–148.

Demaurex, N. (2002). pH homeostasis of cellular organelles. News Physiol. Sci. **17:** 1–5.

Dettmer, J., Hong-Hermesdorf, A., Stierhof, Y.-D., and Schumacher, K. (2006). Vacuolar H$^+$-ATPase activity is required for endocytic and secretory trafficking in *Arabidopsis*. Plant Cell **18:** 715–730.

Di Sansebastiano, G.-P., Paris, N., Marc-Martin, S., and Neuhaus, J.-M. (1998). Specific accumulation of GFP in a non-acidic vacuolar compartment via a C-terminal propeptide-mediated sorting pathway. Plant J. **15:** 449–457.

Di Sansebastiano, G.-P., Paris, N., Marc-Martin, S., and Neuhaus, J.-M. (2001). Regeneration of a lytic central vacuole and of neutral

peripheral vacuoles can be visualized by green fluorescent proteins targeted to either type of vacuoles. Plant Physiol. **126:** 78–86.

Drakakaki, G., Marcel, S., Arcalis, E., Altmann, F., Gonzalez-Melendi, P., Fischer, R., Christou, P., and Stoger, E. (2006). The intracellular fate of a recombinant protein is tissue dependent. Plant Physiol. **141:** 578–586.

Foresti, O., daSilva, L.L., and Denecke, J. (2006). Overexpression of the *Arabidopsis* syntaxin PEP12/SYP21 inhibits transport from the prevacuolar compartment to the lytic vacuole in vivo. Plant Cell **18:** 2275–2293.

Foresti, O., Gershlick, D.C., Bottanelli, F., Hummel, E., Hawes, C., and Denecke, J. (2010). A recycling-defective vacuolar sorting receptor reveals an intermediate compartment situated between prevacuoles and vacuoles in tobacco. Plant Cell **22:** 3992–4008.

Fukao, Y., and Ferjani, A. (2011). V-ATPase dysfunction under excess zinc inhibits Arabidopsis cell expansion. Plant Signal Behav. **6:** 1253–1255.

Gao, D., Knight, M.R., Trewavas, A.J., Sattelmacher, B., and Plieth, C. (2004). Self-reporting Arabidopsis expressing pH and [Ca^{2+}] indicators unveil ion dynamics in the cytoplasm and in the apoplast under abiotic stress. Plant Physiol. **134:** 898–908.

Geldner, N., Dénervaud-Tendon, V., Hyman, D.L., Mayer, U., Stierhof, Y.D., and Chory, J. (2009). Rapid, combinatorial analysis of membrane compartments in intact plants with a multicolor marker set. Plant J. **59:** 169–178.

Gjetting, K.S., Ytting, C.K., Schulz, A., and Fuglsang, A.T. (2012). Live imaging of intra- and extracellular pH in plants using pHusion, a novel genetically encoded biosensor. J. Exp. Bot. **63:** 3207–3218.

Gomez, L., and Chrispeels, M.J. (1993). Tonoplast and soluble vacuolar proteins are targeted by different mechanisms. Plant Cell **5:** 1113–1124.

Gomord, V., Denmat, L.A., Fitchette-Lainé, A.C., Satiat-Jeunemaitre, B., Hawes, C., and Faye, L. (1997). The C-terminal HDEL sequence is sufficient for retention of secretory proteins in the endoplasmic reticulum (ER) but promotes vacuolar targeting of proteins that escape the ER. Plant J. **11:** 313–325.

Herz, J., Hamann, U., Rogne, S., Myklebost, O., Gausepohl, H., and Stanley, K.K. (1988). Surface location and high affinity for calcium of a 500-kd liver membrane protein closely related to the LDL-receptor suggest a physiological role as lipoprotein receptor. EMBO J. **7:** 4119–4127.

Humair, D., Hernández Felipe, D., Neuhaus, J.-M., and Paris, N. (2001). Demonstration in yeast of the function of BP-80, a putative plant vacuolar sorting receptor. Plant Cell **13:** 781–792.

Kang, B.-H., Nielsen, E., Preuss, M.L., Mastronarde, D., and Staehelin, L.A. (2011). Electron tomography of RabA4b- and PI-4Kβ1-labeled trans Golgi network compartments in *Arabidopsis*. Traffic **12:** 313–329.

Kim, H., Kang, H., Jang, M., Chang, J.H., Miao, Y., Jiang, L., and Hwang, I. (2010). Homomeric interaction of AtVSR1 is essential for its function as a vacuolar sorting receptor. Plant Physiol. **154:** 134–148.

Kirsch, T., Paris, N., Butler, J.M., Beevers, L., and Rogers, J.C. (1994). Purification and initial characterization of a potential plant vacuolar targeting receptor. Proc. Natl. Acad. Sci. USA **91:** 3403–3407.

Kornfeld, S. (1992). Structure and function of the mannose 6-phosphate/insulinlike growth factor II receptors. Annu. Rev. Biochem. **61:** 307–330.

Kotzer, A.M., Brandizzi, F., Neumann, U., Paris, N., Moore, I., and Hawes, C. (2004). AtRabF2b (Ara7) acts on the vacuolar trafficking pathway in tobacco leaf epidermal cells. J. Cell Sci. **117:** 6377–6389.

Krebs, M., Beyhl, D., Görlich, E., Al-Rasheid, K.A., Marten, I., Stierhof, Y.-D., Hedrich, R., and Schumacher, K. (2010). *Arabidopsis* V-ATPase activity at the tonoplast is required for efficient nutrient storage but not for sodium accumulation. Proc. Natl. Acad. Sci. USA **107:** 3251–3256.

Lee, G.-J., Sohn, E.J., Lee, M.H., and Hwang, I. (2004). The *Arabidopsis* rab5 homologs rha1 and ara7 localize to the prevacuolar compartment. Plant Cell Physiol. **45:** 1211–1220.

Li, Y.-B., Rogers, S.W., Tse, Y.C., Lo, S.W., Sun, S.S.M., Jauh, G.-Y., and Jiang, L. (2002). BP-80 and homologs are concentrated on post-Golgi, probable lytic prevacuolar compartments. Plant Cell Physiol. **43:** 726–742.

Llopis, J., McCaffery, J.M., Miyawaki, A., Farquhar, M.G., and Tsien, R.Y. (1998). Measurement of cytosolic, mitochondrial, and Golgi pH in single living cells with green fluorescent proteins. Proc. Natl. Acad. Sci. USA **95:** 6803–6808.

Marshansky, V., and Futai, M. (2008). The V-type H$^+$-ATPase in vesicular trafficking: targeting, regulation and function. Curr. Opin. Cell Biol. **20:** 415–426.

Matsuoka, K., Higuchi, T., Maeshima, M., and Nakamura, K. (1997). A vacuolar-type H$^+$-ATPase in a nonvacuolar organelle is required for the sorting of soluble vacuolar protein precursors in tobacco cells. Plant Cell **9:** 533–546.

Matsuoka, K., Matsumoto, S., Hattori, T., Machida, Y., and Nakamura, K. (1990). Vacuolar targeting and posttranslational processing of the precursor to the sweet potato tuberous root storage protein in heterologous plant cells. J. Biol. Chem. **265:** 19750–19757.

Merzlyak, E.M., Goedhart, J., Shcherbo, D., Bulina, M.E., Shcheglov, A.S., Fradkov, A.F., Gaintzeva, A., Lukyanov, K.A., Lukyanov, S., Gadella, T.W., and Chudakov, D.M. (2007). Bright monomeric red fluorescent protein with an extended fluorescence lifetime. Nat. Methods **4:** 555–557.

Miesenböck, G., De Angelis, D.A., and Rothman, J.E. (1998). Visualizing secretion and synaptic transmission with pH-sensitive green fluorescent proteins. Nature **394:** 192–195.

Mollenhauer, H.H., Morré, D.J., and Rowe, L.D. (1990). Alteration of intracellular traffic by monensin; mechanism, specificity and relationship to toxicity. Biochim. Biophys. Acta **1031:** 225–246.

Moseyko, N., and Feldman, L.J. (2001). Expression of pH-sensitive green fluorescent protein in *Arabidopsis thaliana*. Plant Cell Environ. **24:** 557–563.

Nielsen, E., Cheung, A., and Ueda, T. (2008). The regulatory RAB and ARF GTPases for vesicular trafficking. Plant Physiol. **147:** 1516–1526.

Ohgaki, R., van IJzendoorn, S.C., Matsushita, M., Hoekstra, D., and Kanazawa, H. (2011). Organellar Na$^+$/H$^+$ exchangers: Novel players in organelle pH regulation and their emerging functions. Biochemistry **50:** 443–450.

Ordenes, V.R., Moreno, I., Maturana, D., Norambuena, L., Trewavas, A.J., and Orellana, A. (2012). In vivo analysis of the calcium signature in the plant Golgi apparatus reveals unique dynamics. Cell Calcium **52:** 397–404.

Orlowski, J., and Grinstein, S. (2007). Emerging roles of alkali cation/proton exchangers in organellar homeostasis. Curr. Opin. Cell Biol. **19:** 483–492.

Otegui, M.S., Herder, R., Schulze, J., Jung, R., and Staehelin, L.A. (2006). The proteolytic processing of seed storage proteins in *Arabidopsis* embryo cells starts in the multivesicular bodies. Plant Cell **18:** 2567–2581.

Otegui, M.S., Noh, Y.S., Martínez, D.E., Vila Petroff, M.G., Staehelin, L.A., Amasino, R.M., and Guiamet, J.J. (2005). Senescence-associated vacuoles with intense proteolytic activity develop in leaves of *Arabidopsis* and soybean. Plant J. **41:** 831–844.

Paris, N., Rogers, S.W., Jiang, L., Kirsch, T., Beevers, L., Phillips, T.E., and Rogers, J.C. (1997). Molecular cloning and further characterization of a probable plant vacuolar sorting receptor. Plant Physiol. **115:** 29–39.

Paroutis, P., Touret, N., and Grinstein, S. (2004). The pH of the secretory pathway: Measurement, determinants, and regulation. Physiology (Bethesda) **19:** 207–215.

Robinson, D.G., Pimpl, P., Scheuring, D., Stierhof, Y.-D., Sturm, S., and Viotti, C. (2012). Trying to make sense of retromer. Trends Plant Sci. 17: 431–439.

Rogers, S.W., Youn, B., Rogers, J.C., and Kang, C. (2004). Purification, crystallization and preliminary crystallographic studies of the ligand-binding domain of a plant vacuolar sorting receptor. Acta Crystallogr. D Biol. Crystallogr. 60: 2028–2030.

Saint-Jean, B., Seveno-Carpentier, E., Alcon, C., Neuhaus, J.-M., and Paris, N. (2010). The cytosolic tail dipeptide Ile-Met of the pea receptor BP80 is required for recycling from the prevacuole and for endocytosis. Plant Cell 22: 2825–2837.

Saint-Jore, C.M., Evins, J., Batoko, H., Brandizzi, F., Moore, I., and Hawes, C. (2002). Redistribution of membrane proteins between the Golgi apparatus and endoplasmic reticulum in plants is reversible and not dependent on cytoskeletal networks. Plant J. 29: 661–678.

Scheuring, D., Viotti, C., Krüger, F., Künzl, F., Sturm, S., Bubeck, J., Hillmer, S., Frigerio, L., Robinson, D., Pimpl, P., and Schumacher, K. (2011). Multivesicular bodies mature from the trans-Golgi network/early endosome in Arabidopsis. Plant Cell 23: 3436–3481.

Schulte, A., Lorenzen, I., Böttcher, M., and Plieth, C. (2006). A novel fluorescent pH probe for expression in plants. Plant Methods 2: 7–21.

Schumacher, K. (2006). Endomembrane proton pumps: Connecting membrane and vesicle transport. Curr. Opin. Plant Biol. 9: 595–600.

Shimada, T., Fuji, K., Tamura, K., Kondo, M., Nishimura, M., and Hara-Nishimura, I. (2003a). Vacuolar sorting receptor for seed storage proteins in Arabidopsis thaliana. Proc. Natl. Acad. Sci. USA 100: 16095–16100.

Shimada, T., et al. (2003b). Vacuolar processing enzymes are essential for proper processing of seed storage proteins in Arabidopsis thaliana. J. Biol. Chem. 278: 32292–32299.

Sparkes, I.A., Runions, J., Kearns, A., and Hawes, C. (2006). Rapid, transient expression of fluorescent fusion proteins in tobacco plants and generation of stably transformed plants. Nat. Protoc. 1: 2019–2025.

Tamura, K., Shimada, T., Ono, E., Tanaka, Y., Nagatani, A., Higashi, S.I., Watanabe, M., Nishimura, M., and Hara-Nishimura, I. (2003). Why green fluorescent fusion proteins have not been observed in the vacuoles of higher plants. Plant J. 35: 545–555.

Tsuboi, T., and Rutter, G.A. (2003). Multiple forms of "kiss-and-run" exocytosis revealed by evanescent wave microscopy. Curr. Biol. 13: 563–567.

Uemura, T., Kim, H., Saito, C., Ebine, K., Ueda, T., Schulze-Lefert, P., and Nakano, A. (2012). Qa-SNAREs localized to the trans-Golgi network regulate multiple transport pathways and extracellular disease resistance in plants. Proc. Natl. Acad. Sci. USA 109: 1784–1789.

Viotti, C., et al. (2010). Endocytic and secretory traffic in Arabidopsis merge in the trans-Golgi network/early endosome, an independent and highly dynamic organelle. Plant Cell 22: 1344–1357.

Watanabe, E., Shimada, T., Kuroyanagi, M., Nishimura, M., and Hara-Nishimura, I. (2002). Calcium-mediated association of a putative vacuolar sorting receptor PV72 with a propeptide of 2S albumin. J. Biol. Chem. 277: 8708–8715.

Watanabe, E., Shimada, T., Tamura, K., Matsushima, R., Koumoto, Y., Nishimura, M., and Hara-Nishimura, I. (2004). An ER-localized form of PV72, a seed-specific vacuolar sorting receptor, interferes the transport of an NPIR-containing proteinase in Arabidopsis leaves. Plant Cell Physiol. 45: 9–17.

Wee, E.G.-T., Sherrier, D.J., Prime, T.A., and Dupree, P. (1998). Targeting of active sialyltransferase to the plant Golgi apparatus. Plant Cell 10: 1759–1768.

Wilson, D.W., Lewis, M.J., and Pelham, H.R.B. (1993). pH-dependent binding of KDEL to its receptor in vitro. J. Biol. Chem. 268: 7465–7468.

Zhang, G.F., Driouich, A., and Staehelin, L.A. (1993). Effect of monensin on plant Golgi: Re-examination of the monensin-induced changes in cisternal architecture and functional activities of the Golgi apparatus of sycamore suspension-cultured cells. J. Cell Sci. 104: 819–831.